Journal of Applied Polymer Science

Investigations on the polyimides derived from unfunctionalized symmetric cyclopentyl-containing alicyclic cardo-type dianhydride

Fu Li,[1] Wenjun Wan,[1] Jiancheng Lai,[2] Feng Liu,[1] Haixia Qi,[1] Xiaosong Li,[1] Xiaozeng You[2]

[1]College of Chemistry, Jiangxi Provincial Key Laboratory of New Energy Chemistry, Nanchang University, Nanchang 330031, People's Republic of China

[2]State Key Laboratory of Coordination Chemistry, School of Chemistry and Chemical Engineering, Nanjing National Laboratory of Microstructure, Nanjing University, Nanjing 210093, People's Republic of China

Correspondence to: F. Liu (E-mail: liuf@ncu.edu.cn) and X. You (E-mail: youxz@nju.edu.cn)

ABSTRACT: This study presents an investigation on polyimides derived from a unfunctionalized symmetric cyclopentyl-containing alicyclic cardo-type dianhydride with ester linkage 1,1-bis(4-(3,4-dicarboxylbenzoyloxy)phenyl)cyclopentylene dianhydride (BDPCP) that was readily accessed starting from cyclopentanone through two steps in high yield. Two series of polyimides, Cardo-type series (CPI-*x*) and analogous aromatic series (ArPI-*x*) were prepared from condensation of BDPCP and aromatic 3,3′,4,4′-Oxydiphthalic dianhydride with four aromatic diamines, respectively. Comparative studies revealed that CPI polymers show more favorable properties including better solubility in organic solvents, higher transparency with lower cut-off wavelength (λ_0) ranging in 395–375 nm than 425–405 nm, lower water absorption ranging in 0.66–1.14% and surface energy 23.71–32.77 mN/m than 1.01–1.28% and 29.52–41.99 mN/m of ArPI analogs. Meanwhile, CPI series exhibit considerable mechanical properties with tensile strengths ranging in 87.6–102.9 MPa, elongations at break 6.6–8.9%. Owing to the moderate strain in cyclopentyl ring, CPI series retain good thermal properties with the glass transition temperature (T_g) in the range of 217–271°C. Dynamic dielectric measurement revealed that Cardo-type dianhydride BDPCP endows CPI-4 film with lower dielectric constant (ε') 3.34 at 1 MHz and 25°C and dielectric loss (ε'') 0.0064 at 1 kHz and 25°C than 3.49 and 0.013 for ArPI-4 film. © 2015 Wiley Periodicals, Inc. J. Appl. Polym. Sci. **2015**, *132*, 42670.

KEYWORDS: alicylic polyimide; cardo-type dianhydride; cyclopentyl; dynamic dielectric analysis; glass transition temperature

Received 26 February 2015; accepted 27 June 2015

DOI: 10.1002/app.42670

INTRODUCTION

Aromatic polyimides (PIs), as one well-known class of high-performance materials, are widely used due to their high thermal stability, good chemical and irradiation resistance, and excellent mechanical and electrical properties.[1,2] These outstanding properties are, in a degree, attributed to the charge transfer complex (CTC) formed between the alternating electron-donating diamine segments and electron-accepting dianhydride segments in the polymer backbones, which further leads to the dense chain packing. Conversely, CTC and dense chain packing have been believed to account for the poor processing properties, low transparence, and high dielectric constant of PIs, which restricted their applications in advanced microelectronics and optoelectronics.[3–5] Hence, considerable research effort in structural modification aiming at reducing CTC and lowering the chain packing has been made to overcome the limitations of aromatic PIs. Early modification approaches included the introduction of flexibilizing groups, bulky substituents, asymmetric units including isomeric structure into the main chains.[6–11] By introducing these solubilizing moieties which typically inhibit the formation of CTC and chain packing, the improved processability of PIs could be obtained such as organosolubility and melt processing performance. Meanwhile, the sacrifices in thermal and mechanical stability were invariably accompanied with these modification advantages. Recently, semi or fully aliphatic, alicyclic including heterocyclic, and fluorinated structures have attracted intense research interests in modifying PIs due to their remarkable improvement on optical and dielectric properties.[12–19] Owing to the broken aromatic conjugation, inhibited CTC, and lowered molar polarizability, some desired properties such as the improved processability, alleviated coloration, and reduced dielectric constant could be achieved in these modified PIs. Nevertheless, these approaches still encounter the trade-off problem of the thermal, mechanical properties in exchange with

Additional Supporting Information may be found in the online version of this article.

the gained optical, dielectric properties. Therefore, it remains an important consideration for any modification approach to minimize the trade-off in the inherent excellent thermal and mechanical properties in pursuit of improving other practical properties of PIs.

Cardo-type PIs were initially proposed and investigated as tractable polymers with better solubility and melting processability.[20–23] Considerable research effort has of late expanded to the more intensive evaluation of the influences of Cardo structure to the general properties and specific application of Cardo PIs.[24–28] It has been found that the incorporation of Cardo structure into the main chains of PIs helps improve not only the processability but also optical and dielectric properties, and more importantly, the thermal stabilities were greatly maintained. Although some other scattered methods were reported, Cardo-type monomers could be generally achieved by the key intermediate Cardo diols like bisphenols that are obtained by condensation of phenol with various cycloketone in high yield, reacting with anhydride or amine precursors to finally offer the dianhydrides or diamines. Because of the high efficiency of synthesizing the intermediate Cardo diols and the readiness of the subsequent synthetic processes, the Cardo-type monomers accessible with plentiful structural variations could be considered as the facile strategic choices that bear the industrially important cost-effectiveness and readiness of scale-up. The application of Cardo structure has also been under investigation in the field beyond PI and the environmentally benign synthetic routes of the Cardo diol were explored.[29–31] The improved processability, optical, and dielectric properties of Cardo-type PIs can be explained as that the cycloaliphatic ring and C—O linkage in Cardo structure breaks the aromatic conjugation and contributes to the flexibility in the polymer backbone as well, and simultaneously, the thermal and mechanical properties are greatly guaranteed and maintained due to the reinforced polymer backbone rigidity endowed by the disubstituted aromatic rings in the Cardo-structure.

Recently, with the widespread development of advanced microelectronics and optoelectronics, it is increasingly important to establish several kinds of dependable PIs that meet the key industrial dielectric and optical properties requirements and are also readily accessible.[32,33] Cardo-type PIs possess comparable dielectric and optical properties with other PIs like those containing alicyclic or fluorinated structures, and enjoy the advantageous minimized trade-off in thermal and mechanical properties, and are particularly ready to prepare from commonly accessible industrial chemicals like cycloketone and phenol. Therefore, it is of practical significance to comprehensively evaluate the Cardo-type PIs derived from readily accessible cycloketone such as cyclohexanone and cyclopentanone. Different kinds of Cardo-type PIs based on cyclohexanone and functionalized cyclohexanone have been investigated.[34–36] We have recently studied the thermal, optical, and dielectric properties of a series of Cardo-type PIs derived from a novel fluorinated Cardo-type diamine starting from cyclopentanone and phenol.[37] As a continuation, we herein present an unreported unfunctionalized Cardo-type dianhydride prepared from cyclopentanone and phenol. The pivotal consideration of this study is to evaluate the unfunctionalized (unfluorinated and without pendent groups) Cardo-type PIs derived from this readily accessible alicyclic Cardo dianhydride with the most simplified preparation procedure. We believe that this approach is practically valuable due to its industrially beneficial lower production cost than functionalized series, which would otherwise inevitably make the real fabrication of PI materials a demanding task due to their sophisticated and thus highly expensive synthetic processes involving the functionalization of the monomers. Rare literature illustrated the detailed dielectric properties of the PIs derived from alicyclic Cardo-type dianhydride. A particular emphasis in this work will be placed on the comparative study of the dielectric properties of the alicyclic Cardo dianhydride derived PIs under varied temperature and frequency using dynamic dielectric measurement. Meanwhile, the general comparative studies of the thermal, mechanical, optical, and surface properties between PIs from the new dianhydride and PIs from a commercial dianhydride 3,3′,4,4′-oxydiphthalic dianhydride (ODPA) have been performed to explore the structure–properties relationships.

EXPERIMENTAL

Materials

Cyclopentanone, 3-mercaptopropionic acid, and phenol were purchased from Sinopharm Chemical Reagent, China and used as received. Trimellitic anhydride chloride (TMAC), ODPA, 2,2′-dimethyl-4,4′-diaminobiphenyl (DMB), 1,3-bis(4-aminophenoxyl)benzene (1,3,4′-APB), 1,4-bis(4-aminophenoxyl)benzene (1,4,4′-APB), and 4,4′-oxydianiline (ODA) were commercially obtained and dried in a vacuum oven at 80°C overnight prior to use. Commercially available *N*-methyl-2-pyrrolidinone (NMP), m-cresol, *N*,*N*-dimethylacetamide (DMAc) were purified by vacuum distillation over P_2O_5 and *N*,*N*-dimethylformamide (DMF) was purified by vacuum distillation over CaH_2 and then stored over 4 Å molecular sieves prior to use. Other commercially available materials were used without further purification.

Measurement

IR spectra with resolution of 0.5 cm^{-1} were recorded on a Perkin Elmer Fourier Transform Infrared spectrometer Perkin Elmer SP one FT-IR with KBr pellets if not specified otherwise. ^{1}H-NMR and ^{13}C-NMR spectra were measured on a Bruker DRX 400 spectrometer with $CDCl_3$ and $(CD_3)_2SO$-d_6 as the solvent and tetramethylsilane as the internal reference. The melting points were measured with a microscopic melting point apparatus SGW-X4 (Shanghai Science Apparatus, China) using capillary samples. Elemental analyses were performed on a Perkin-Elmer-240 (II) C, H, N analyzer. Wide-angle X-ray diffraction (WAXD) measurement was performed at 25°C on a Bede XRD Di system, using graphite-monochromatized Cu-Kα radiation ($\lambda = 0.15405$ nm). Ultraviolet visible (UV–vis) spectra of the polymer films were recorded on a Shimadzu UV–visible spectrophotometer UV-2450. Thermogravimetric analysis (TGA) measurements were conducted with a Perkin-Elmer TGA-2 in flowing nitrogen or in air at a heating rate of 10°C/min. Dynamic mechanical analysis was conducted with DMA Q800 V20.22 Build 41 using tensile mode at the frequency of 1 Hz

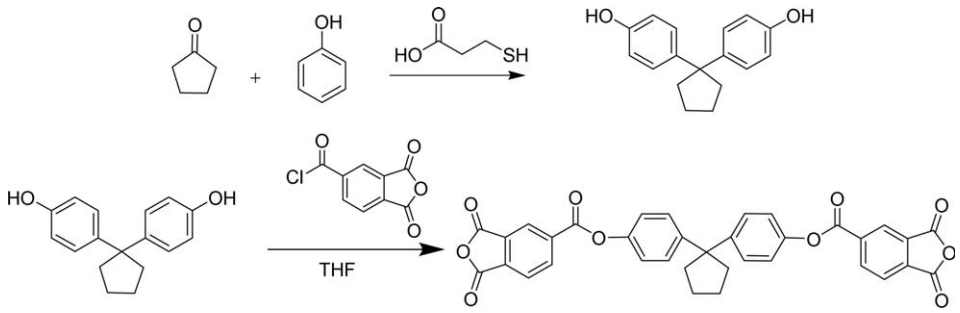

Scheme 1. The general synthetic route of BDPCP.

and heating rate of 3°C/min. Coefficients of thermal expansion (CTEs) of the films were detected in the optical dilatometer DIL-806 dilatometer (Baehr-Thermoanalyse GmbH, Germany) with the heating rate of 10 K/min and measurement precision of 0.1 μm. An Instron universal tester model 1122 (GB/T1040.1–2006) was used to study the stress–strain behavior of the film samples at room temperature with a stretching rate of 2.5 mm/min, and the data were the average value of five experiments except for the maximum and the minimum value. Contact angle measurements were performed using Drop Master 300 Contact AM system (Kyowa Interface Science, Saitama, Japan). Dielectric spectroscopy measurements of the polymer films with the temperature variation in the range of 150–520 K and the frequency variation in the range of 1–10^7 Hz have been performed using a Novocontrol Dielectric Spectrometer (GmbH Germany), CONCEPT 40. Polymer film electrodes with diameter of 20 mm and thickness of 40–80 μm having gold plated were placed in a flat parallel plate capacitor, and the amplitude of AC applied voltage was 1 V.

Monomer Synthesis

Experimentally, a novel unfunctionalized alicyclic Cardo dianhydride monomer 1,1′-bis(4-(3,4-dicarboxylbenzoyloxy)phenyl) cyclopentylene dianhydride (BDPCP) was prepared starting from cyclopentanone and phenol through two steps, as shown in Scheme 1.

The Synthesis of 1,1-Bis(4-hydroxyphenyl) Cyclopentane

A mixture of cyclopentanone (4.21 g, 0.05 mol), phenol (18.5 g, 0.2 mol), 3-mercaptopropionic acid (0.52 mL), and 45 mL hydrochloric acid/acetic acid (volume ratio 2 : 1) was placed in a 250 mL three-necked flask equipped with a mechanical stirrer and reacted at room temperature for 24 h. The obtained purple precipitate was washed with hot water, dissolved in 2 mol/L aqueous sodium hydroxide solution, acidized with concentrated hydrochloride acid to offer the precipitated solid, which was subsequently washed with water twice, and dried at 60°C under vacuum. The crude product was then recrystallized from toluene twice to afford pink crystals (9.34 g, 73.6%). m.p.: 153–155°C. The IR spectrum exhibited absorptions at 3253 (—OH stretching); 3033 (Ar-H stretching); 2969, 2866 (alicyclic C—H stretching). ^{1}H-NMR (DMSO-d_6, δ, ppm): 9.03 (s, 2H, 5), 7.04 (d, 4H, 3), 6.59 (d, 4H, 4), 2.14 (t, 4H, 2), 1.56 (m, 4H, 1). ^{13}C-NMR (DMSO-d_6, δ, ppm): 155.31 (s, 7), 139.72 (s, 4), 128.03 (s, 5), 115.12 (s, 6), 54.19–54.06 (m, 3), 38.48 (s, 2), and 22.84 (s, 1). Elemental analysis (%): calculated: C, 80.28; H, 7.13; O, 12.58; found: C, 80.16; H, 7.23%; O, 12.61. The IR, ^{1}H-NMR, and ^{13}C-NMR spectra of 1,1-bis(4-hydroxyphenyl) cyclopentane (BHCP) were shown in Supporting Information Figures S1, Figure S2, and Figure S3, respectively.

The Synthesis of 1,1-Bis(4-(3,4-dicarboxylbenzoyloxy)phenyl)cyclopentylene Dianhydride

A new Cardo dianhydride containing alicyclic five-membered ring structure and ester linkage 1,1-bis(4-(3,4-dicarboxylbenzoyloxy)phenyl)cyclopentylene dianhydride (BDPCP) was achieved by reacting BHCP with TMAC as described herein: BHCP (5.09 g, 0.02 mol) was dissolved in a mixed solvent of 40 mL anhydrous tetrahydrofuran (THF) and pyridine (3.17 g, 0.04 mol) in a three-necked round bottom flask with a nitrogen inlet. TMAC (7.4 g, 0.04 mol) dissolved in 60 mL THF was gradually added and reacted at room temperature overnight. Then the mixture was filtered to remove pyridine hydrochloride, and the obtained solution was concentrated in vacuum. The precipitated solids were purified by recrystallization in the mixture of acetic anhydride and toluene (volume ratio: 1 : 6) twice to yield white crystals (10.00 g, 83%). m.p.: 195–197°C. The IR spectrum was shown in Supporting Information Figure S4. The ^{1}H-NMR spectrum ($CDCl_3$ as solvent) and ^{13}C-NMR spectrum (DMSO-d_6 as solvent) of BDPCP were shown in the Figures 1 and 2. The IR spectrum (cm^{-1}) exhibited absorptions at 2957, 2871 (alicylic C—H stretching); 1859, 1783 (anhydride C=O stretching); 1741 (ester C=O stretching); 1229 (C—O—C stretching). ^{1}H-NMR ($CDCl_3$, δ, ppm): 8.78 (s, 2H, 7), 8.73–8.60

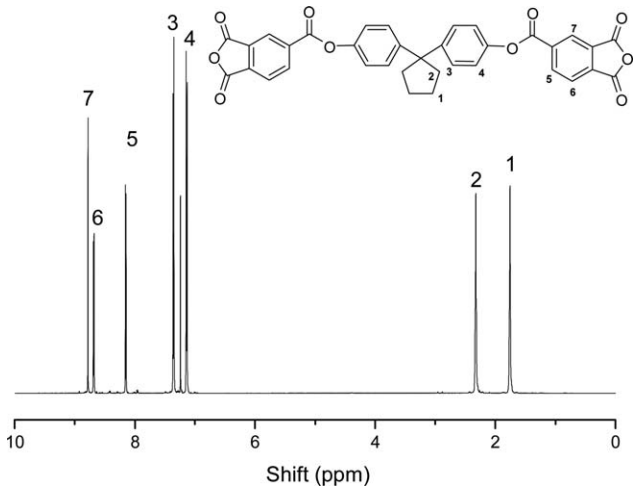

Figure 1. The ^{1}H-NMR spectrum of BDPCP.

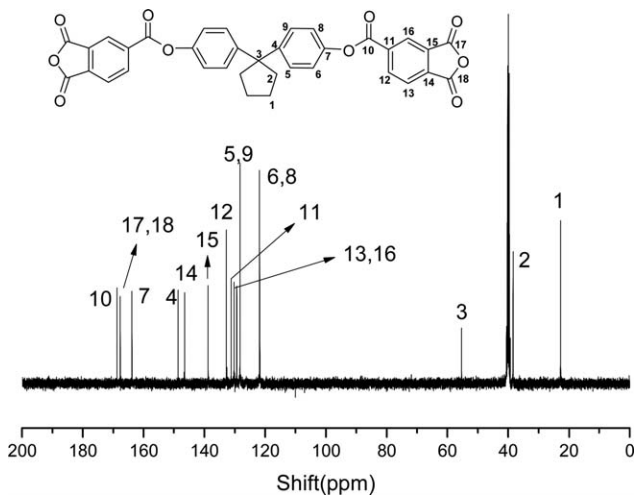

Figure 2. The ^{13}C-NMR spectrum of BDPCP.

(m, 2H, 6), 8.15 (d, $J = 7.9$ Hz, 2H, 5), 7.35 (t, $J = 8.1$ Hz, 4H, 3), 7.14 (d, $J = 8.6$ Hz, 4H, 4), 2.33 (s, 4H, 2), 1.76 (s, 4H, 1). ^{13}C-NMR (DMSO-d_6, δ, ppm): 168.73 (s, 10), 167.70 (s, 17/18), 163.78 (s, 7), 148.65 (s, 4), 146.50 (s, 14), 138.72 (s, 15), 132.73 (s, 12), 131.12 (s, 11), 130.21 (s, 13/16), 129.34 (s, 5/9), 121.83 (s, 6/8), 55.30 (s, 3), 38.39 (s, 2), 22.73 (s, 1). Elemental analysis (%): calculated: C, 69.77; H, 3.68; O, 26.55; found: C, 70.02; H, 3.65; O, 26.33.

Preparation of the Polyimide Films

Eight polyimide films were prepared by conventional two-step polycondensation from BDPCP and ODPA with four commercial diamines, DMB, 1,4,4′-APB, 1,3,4′-APB, and ODA, respectively, and coded as CPI − x (x = 1–4) and ArPI − x(x = 1–4) correspondingly. The synthesis of the polyimides was shown in Scheme 2. CPI-4 (BDPCP/ODA) is used as an example to illustrate the general synthetic process for preparing the polyimides. Diamine ODA (0.4005 g, 2 mmol) was dissolved in 7.3 g dried DMAc in a 25 mL flask under nitrogen, then 1.2051 g (2 mmol) BDPCP was added to the solution in one portion. The mixture was stirred at room temperature for 12 h to form a viscous poly(amic acid) solution. The poly(amic acid) solution was then poured onto a glass plate, and placed in an 80°C oven for 5 h to release the casting solvent. The half-dried poly(amic acid) film was further thermally cured and imidized by sequential heating at 150°C for 1 h, 200°C for 1 h, 250°C for 1 h, and 280°C for 2 h. After being soaked in boiled water, a flexible polyimide film of CPI-4 was released from the glass surface. The synthesis of the above PIs was shown in Scheme 2. IR (cm^{-1}, film): 1781, 1717 (imide carbonyl asym. and sym. stretching), 1366 (C—N stretching), and 724 cm^{-1} (imide ring deformation). Representative IR spectra of the film were shown in Supporting Information Figure S5. All the ensuing polymer property measurements were performed using PI film specimens.

RESULTS AND DISCUSSON

The Solubility, WAXD, and Optical Properties of the Polymers

The solubility of the PIs was tested in various solvents and the results are summarized in Table I. Most of the PI films obtained in this study were readily soluble in typical polar solvents such as 3-methylphenol (m-Cresol), *N*-methyl-2-pyrrodidon (NMP) at room temperature. The Cardo-type series CPI show considerably better solubility than the aromatic series ArPI. In particular, CPI-2 and CPI-3 show good solubility in common organic solvents like chloroform and tetrahydrofuran. The better solubility of CPI-x could be attributed to synergistic effect of Cardo structure and ester linkage in the backbone of polymer, which increased the polymer backbone flexibility, enlarged the interchain distance, decreased the chain packing, and the interchain CTC.[24,38] Further evidence could be obtained from wide angle

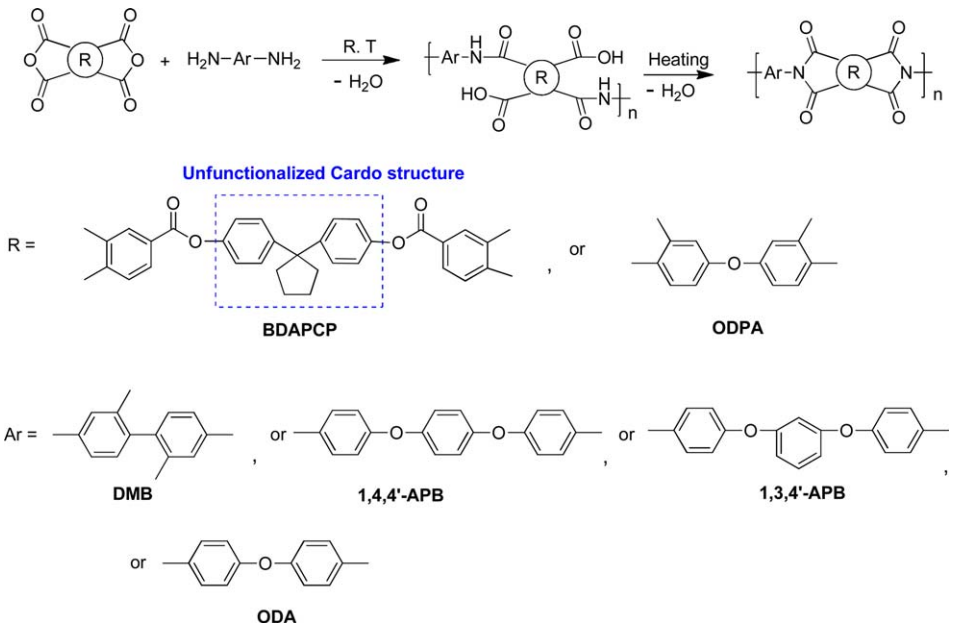

Scheme 2. The synthesis of the polyimide films. [Color figure can be viewed in the online issue, which is available at wileyonlinelibrary.com.]

Table I. The Solubility, *d*-Spacing Value, and Optical Properties of the Polyimide Films

			Solubility[a]							WAXD[b]		Optical properties	
Polymer	Dianhydride	Diamine	DMSO	THF	CHCl3	m-Cresol	DMAc	NMP	DMF	2θ (°)	*d*-Spacing (Å)	T_{500} (%)[c]	λ_0 (nm)[d]
CPI-1	BDPCP	DMB	–	–	–	+	+	+	+h	16.80	5.27	72.6	395
CPI-2	BDPCP	1,4,4′-APB	+	+	+	+	+	+	+	16.00	5.53	83.5	375
CPI-3	BDPCP	1,3,4′-APB	+	+	+	+	+	+	+	15.56	5.69	82.4	378
CPI-4	BDPCP	ODA	+h	+h	+h	+	+	+	+	16.30	5.43	76.2	390
ArPI-1	ODPA	DMB	-	-	-	+h	+h	+h	-	18.66	4.75	71	425
ArPI-2	ODPA	1,4,4′-APB	+h	+h	+h	+	+	+	+	17.16	5.16	78.8	405
ArPI-3	ODPA	1,3,4′-APB	+h	+h	+h	+	+	+	+	17.22	5.14	76.2	415
ArPI-4	ODPA	ODA	-	-	-	+h	+h	+	+h	17.82	4.97	74.2	418

[a] Qualitative solubility measured with 100 mg of the polymer in 2mL of solvent. +, soluble at room temperture; +h, soluble after heating; −, insoluble.
[b] The most prominent WAXD peak in the amorpous glassy polymer spectra was adopted to calculate the *d*-spacing value according to Bragg's equation: $2d\sin\theta = n\lambda$, n = 1, λ = 1.54 Å.
[c] Transmittance at 500 nm.
[d] dUV-vis cutoff wavelength.

X-ray diffraction (WAXD) measurement. Average interchain spacing distance (*d*-spacing) values were calculated from the most prominent WAXD peak in the amorphous glassy polymer spectra based on Bragg's equation. As seen in WXAD spectra in Supporting Information Figure S6, all the films presented amorphous state, exhibiting *d*-spacing value ranging from 4.75 to 5.69 Å, as summarized in Table I. The *d*-spacing value of CPI-*x* is bigger than analogous ArPI-*x*, indicating a larger interchain distance. This result theoretically infers that compared with aromatic analogs, Cardo series with enlarged interchain distance were more readily to be solubilized. The solubility of PIs with different diamine structures was shown in the decreasing order of 1,4,4′-APB, 1,3,4′-APB > ODA > DMB, which was in agreement with the decreasing molecular flexibility degree order of these diamines.

The UV–Vis spectra of all CPI films and ArPI films were shown in Figures 3 and 4, and the transmittance at 500 nm (T_{500}) and UV cutoff wavelength (λ_0) were abstracted into Table I. By comparison, the CPI-*x* enjoys higher optical transparency than its analogous ArPI-*x*. For instance, CPI-2 and CPI-3 show T_{500} over 80% and λ_0 below 380 nm, which meet the applicable properties criterion for advanced optoelectronics. Whereas, T_{500} values of the analogous aromatic series ArPI-*x* are lower than 80% and λ_0 values above 400 nm. The optical transparency differences between CPI and ArPI series are explainable by the decreased CTC formation in CPI films that results from the alicyclic cyclopentyl ring structure that breaks the conjugation of the polymer chain and thus segments the charge transfer pathway. The effects of different diamine structure on the transparency of the polymer films are similar to those on the solubility of the polymers. The more flexible diether-linked diamines 1,4,4′-APB, 1,3,4′-APB generate higher T_{500} and lower λ_0 than do the other two diamines, among which ODA offers polymer higher transparency than the strained dimethyl substituted biphenyl diamine DMB does.

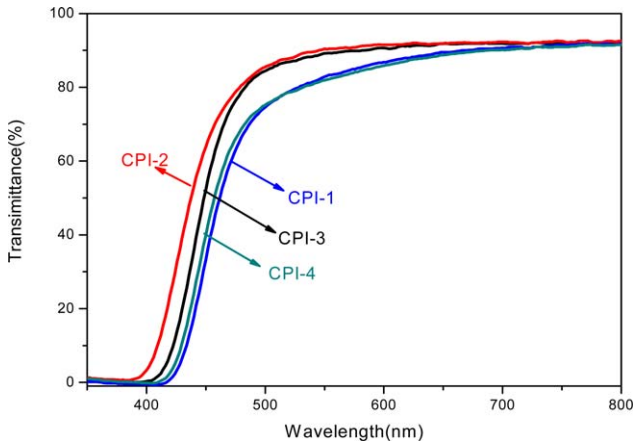

Figure 3. The UV–Vis spectra of CPI films. [Color figure can be viewed in the online issue, which is available at wileyonlinelibrary.com.]

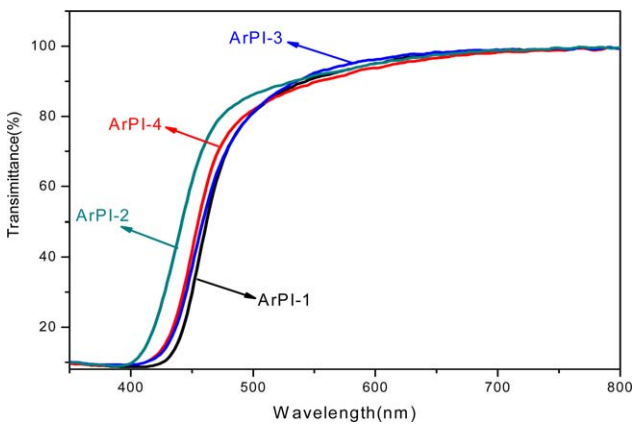

Figure 4. The UV–Vis spectra of ArPI films. [Color figure can be viewed in the online issue, which is available at wileyonlinelibrary.com.]

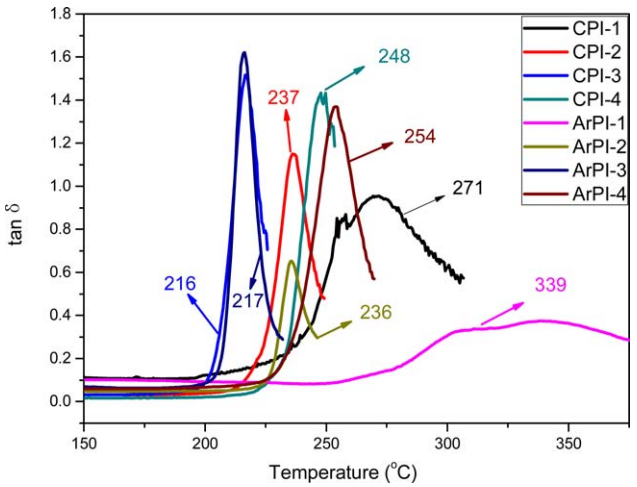

Figure 5. DMA curves of the polyimides. [Color figure can be viewed in the online issue, which is available at wileyonlinelibrary.com.]

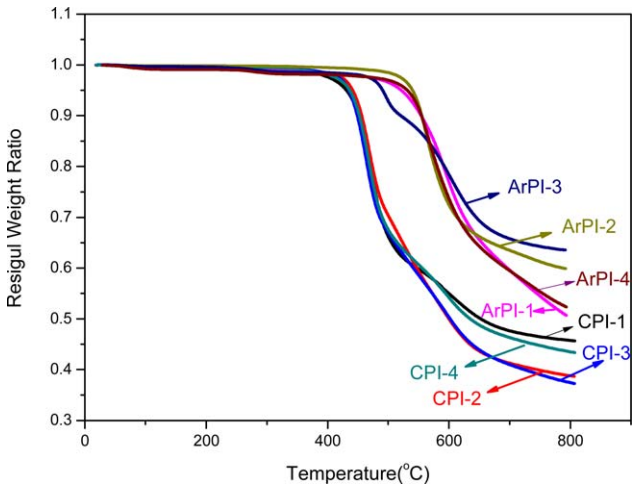

Figure 6. TGA curves of the polyimide films. [Color figure can be viewed in the online issue, which is available at wileyonlinelibrary.com.]

Thermal Properties of the Polymers

The DMA (dynamic mechanical analysis) and TGA (thermogravimetric analysis) curves were derived to evaluate the thermal properties of the polyimides films, as shown in Figures 5 and 6, and the results are summarized in Table II. T_g values of CPI series are in the range of 217°C–271°C, whereas those of the aromatic analogs ranging in 216°C–339°C. Except for the case of DMB as condensation diamine, the Cardo series exhibit generally comparable values to their aromatic analogs in terms of glass transition temperature. For instance, the CPI-4 has T_g value of 248°C while the T_g of corresponding ArPI-2 is 254°C, and T_g values 237°C and 217°C of CPI-2 and CPI-3 compare to 236°C and 216°C of their aromatic analogs. These close values of T_g between the two series suggest that the Cardo-structure serves well to retain the good thermal stability of aromatic PIs, further indicating that the introduction of facile ester linkage does not harm the thermal stability of the polymer materials. That could be partly attributed to the presence of two substituted aromatic phenyl groups on the cyclopentyl. Meanwhile, even though the cyclopentyl structure is classified as thermodynamically stable five-membered ring, it actually has certain molecular steric strain compared with larger ring like cyclohexyl, and its steric strain become intensified due to the disubstitution of bulky group on the carbonyl carbon, which further adds to the rigidity of polymer backbone and so contributes to thermal stability of the polymer. Molecular mechanical analysis found the presence of larger torsional strain in cyclopentyl ring than in cyclohexyl ring.[39] Our previous work showed that cyclopentyl structure leads to higher T_g than cyclohexyl structure does to Cardo-type PIs.[40] The highly restrained and rigid

Table II. The Thermal, Mechanical, and Surface, Moisture Uptake Properties of the PIs

	Thermal properties					Mechanical properties[a]					
Polymer	T_g (°C)[b]	T_{d5} (°C)	T_{d10} (°C)	Char yield (%)[c]	CTE (ppm/K)[d]	TS (MPa)	EB (%)	TM (GPa)	θ (°)[e]	γ_s (mN/m)[f]	Water absorption (%)[g]
CPI-1	271	431	451	47.6	32.1	102.9	6.8	2.62	81.8	32.77	1.14
CPI-2	237	441	456	41.2	54.1	98.3	8.9	2.24	87.2	27.63	0.66
CPI-3	217	434	449	41	61.1	97.2	8.3	2.31	91.6	23.71	0.76
CPI-4	248	436	452	46.3	49	76.2	6.6	2.23	86.0	28.74	0.69
ArPI-1	339	521	554	59.6	28.7	138.4	7.9	2.86	72.9	41.99	1.28
ArPI-2	236	540	555	63.5	38.5	115.7	9.7	2.35	78.9	35.70	1.17
ArPI-3	216	490	520	65.8	43.9	97.5	6.7	2.42	85.1	29.52	1.31
ArPI-4	254	531	555	59.5	33.2	87.6	9.5	2.53	77.9	36.69	1.01

[a] TS, tensile strength; EB, elongation at break; TM, tensile modulus.
[b] Glass transition temperature (T_g) was measured by DMA at a heating rate of 10°C/min.
[c] Residual weight percentage at 800°C in N_2.
[d] The in-plane coefficients of thermal expansion.
[e] Equilibrium contact angle was measured at ambient temperature and double distilled water as solvent for a time period of 120 s depending on the stability of the drop, and the data were the average value of 10 experiments.
[f] Surface energy is obtained indirectly from the water contact angle by Owen equation.
[g] Water absorption (%) = $(W - W_0/W_0) \times 100\%$; where W is the weight of polymer sample after immersed in water for 96 h at room temperature and W_0 the weight of polymer sample after being dried in vacuum at 100°C for 8 h.

dimethyl substituted biphenyl structure leads to high T_g of DMB-derived CPI-1 (271°C) and the glass transition is not seen for ArPI-1. The secondary relaxation peak at high temperature (339°C) for ArPI-1 may be attributed to the synergistic stiffening effect of the rigid dimethyl substituted biphenyl structure coupled with aromatic dianhydride partner. The polymer chain torsion arising from the molecular strain in DMB moiety tends to be relieved by the thermal fragmentation of the substituted methyl groups at high temperature, which should be the reason of what was observed from TGA data that the T_{d5} and T_{d10} of DMB-derived polymers drop back to the same range as or even exhibit lower value than those of the polymers derived from the other tested diamines. The thermal decomposition stabilities as denoted by T_{d5} and T_{d10} of Cardo series are understandably lower than aromatic series due to the presence of pyrolytically less stable alicyclic cyclopentyl structure and ester linkage in BDPCP moiety, as explicitly shown in Figure 6. Owing to the flexible ester linkage and alicyclic cyclopentyl structure in polymer backbone, CPI series are more inclined to expand when heated than ArPI series. CPIs possess CTE (coefficient of thermal expansion) values of 32.1–61.1 ppm/K during the temperature scope of 25–300°C, while CTE values of ArPI series ranging in 28.7–43.9 ppm/K, as shown in Supporting Information Figure S7. It is found that the DMB is effective to upgrade the thermal dimension stability of both Cardo and aromatic PI films, as shown by the strikingly lower CTE value of CPI-1 (32.1 ppm/K) and ArPI-1 (28.7ppm/K). That could be attributed to the stiffening effect of polymer chain by the strained DMB structure. Different diamine structures influence the thermal properties of the polymers in a similar way but in reverse order as they do to the solubility and optical properties. The thermal properties of PIs with different diamines exhibit the decreasing order as DMB > ODA > 1,4,4′-APB > 1,3,4′-APB. As an important electronic insulating property, CTE of PI was believed to be influenced by the molecular weight, polymer chain rigidity, and crystallinity.[40] Actually, CTC plays an important role in offering the interchain locking force, so stronger CTC leads to greater dimension stability. It is recently reported that by enlarging the electron-donating properties using alicyclic diamine and coupling with rigid electron-accepting aromatic dianhydride partner, CTE of PI could be lowered to be comparable to that of copper foil.[41] Relatively high CTE results of CPI series in this work are, in a degree, associated with the decreased CTC of PIs containing Cardo structure and ester linkage.

Mechanical and Surface Properties of the Polymers

Mechanical properties of the PIs were summarized in Table II. All the amorphous PIs afforded flexible and tough films, and their stress–strain curves were shown in Supporting Information Figure S8. CPI-*x* series show tensile strengths at break of 87.6–102.9 MPa, elongation at break of 6.6–8.9%, and tensile modulus of 2.23–2.62 GPa. By contrast, ArPI-*x* series showed tensile strengths of 76.2–138.4 MPa, elongation at break of 6.7–9.7%, and tensile modulus of 2.23–2.86 GPa. In terms of tensile strengths and tensile modulus, CPI series display a more concentrative range than ArPI series, but with smaller values. The larger tensile strengths and tensile modulus of ArPI series could be accounted for by their more rigid aromatic structure than CPI series. Both series followed the tendency of diamine structure variation with the decreasing order of DMB > 1,4,4′-APB > 1,3,4′-APB > ODA in terms of tensile strengths and tensile modulus, which generally match the decreasing order of the used diamines' rigidity degree except for ODA. Based on molecular rigidity, ODA should follow DMB as shown by the thermal properties comparison. The unusual mechanical properties of ODA-based PIs in this study may be attributed to their poor chain entanglement for ODA is not as flexible as 1,3,4′-APB or 1,4,4′-APB and it also lacks the pendent substitutents like methyl in DMB that offer involvement to interchain entanglement. It is also seen that for two rigid diamines DMB and ODA, elongation values of aromatic series (ArPI-1 and ArPI-4) are larger than those of Cardo series (CPI-1 and CPI-4). But for the PI films derived from flexible diamines 1,3,4′-APB or 1,4,4′-APB, exchanging aromatic dianhydride with cardo dianhydride helps to increase the toughness of films as suggested by the larger value of elongation of CPI-2 and CPI-3 than the analogous ArPI-2 and ArPI-3. These results may be partly understood as the larger chain slippage effect of CPIs in plastic deformation during stretching tests. The larger chain slippage may originate from the decreased interchain forces of CPIs by inhibiting CTC effect of the Cardo dianhydride coupled with flexible diamine partners.

The contact angles (θ) of the thermally imidized PI films against water are listed in Table II, which shows that the θ values of the two series are in the range of 81.8–91.6° and 75.9–85.1°, respectively. Supporting Information Figure S9 depicted the profiles of a droplet on the CPI and ArPI series surface. The larger θ values of CPI films than analogous ArPI films indicate that exchanging aromatic dianhydride with Cardo dianhydride increases the hydrophobicity of PI films due to the presence of alicyclic cyclopentyl Cardo structure. Based on measured contact angles, values of surface energy (γ_s) of PI films were obtained using the equation: $1+\cos\ \theta = 2(\gamma_s/\gamma_l)^{1/2}\exp[-\beta(\gamma_l-\gamma_s)]^2$, where, β is a constant with a value of 0.0001247 $(m^2/mJ)^2$, γ_s and γ_l are the surface energy of the solid and the surface energy of the testing liquid, respectively. The γ_s values of Cardo CPIs in Table II demonstrate a corresponding decrease to those of aromatic ArPIs. Large contact angle and low surface free energy of the Cardo series may be due to the less polar alicyclic cyclopentyl with tetrahedral sp^3 hybridized carbon than aromatic ring with planar sp^2 hybridized carbon, which decreases the material's affinity towards water, so reducing the surface tension and making the surface more hydrophobic. Additionally, the hydrophobic alicyclic cyclopentyl groups lead to the better moisture barrier properties of the Cardo series with the lower water uptake ranging in 0.66–1.14% than 1.01–1.31% of the analogous aromatic series. Compared with aromatic series, the Cardo series show greater practical reliability to withstand long-term humid working environment for optoelectronics and microelectronics application.

Dielectric Properties of the Polymers

To investigate the influence of Cardo cyclopentyl structure to the dielectric properties, thermally imidized PI films (CPI-4 and ArPI-4) were evaluated in terms of dielectric constant (ε'), dielectric loss (ε'') with variation of frequency and temperature.

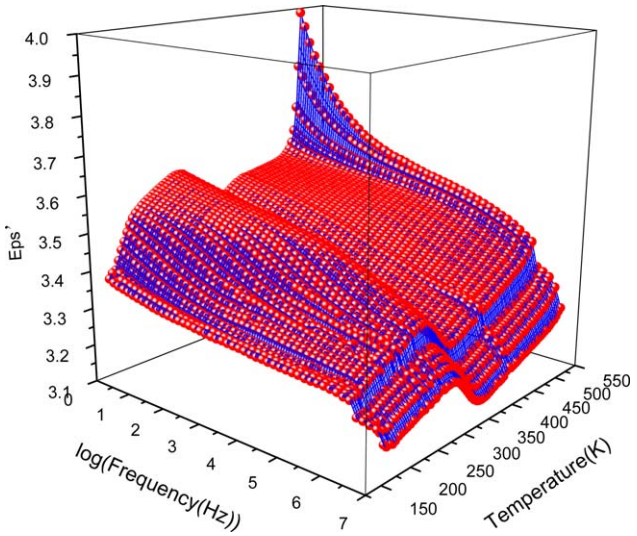

Figure 7. The dielectric constant versus frequency and temperature for CPI-4. [Color figure can be viewed in the online issue, which is available at wileyonlinelibrary.com.]

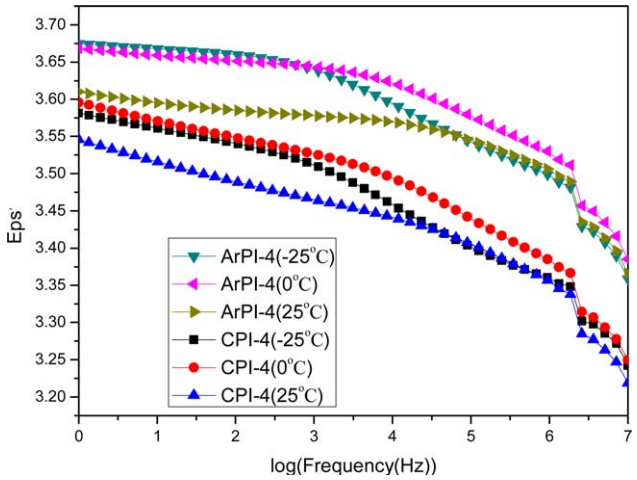

Figure 9. Dielectric constant (ε') versus frequency of polyimide films CPI-4 and ArPI-4. [Color figure can be viewed in the online issue, which is available at wileyonlinelibrary.com.]

The three-dimensional diagram of dielectric constant (ε') versus frequency and temperature for CPI-4 and ArPI-4 shows in Figures 7 and 8, which show the general increasing tendency of ε' with decreasing frequency and increasing temperature for both samples. In terms of the effects of the structural variation, the ε' value of the polymer increases with increasing polarizability and decreasing free volume.

One can see in these figures that with increasing temperature ε' value presents a rapid increase at low temperature that was attributed to the flexibilizing of the low-temperature stiffened polymer backbone and the concomitant polarizability increase, and then an appreciable transition for both samples with an initial increase followed by a decrease in the range of 250–300 K, as reported by our previous work.[40] The decrease of ε' value in this transition may be associated with the variation of free volume that would increase to an appropriate extend due to the expansion of the flexibilized polymer chain as the temperature further increases. After the transition temperature range, the subsequent trend of ε' value variation follows a gradual increase with increasing temperature due to the increasing mobility of polymer chain that contribute to the increased orientational polarization of the dipoles along the polymer chain. Figure 10 depicts the variation of ε' with increasing frequency at three selected temperature, −25°C, 0°C, and 25°C whose coverage corresponds to the above transition range of ε' versus temperature. The transition is explicitly revealed in Figure 9 by the ε' value increasing from −25°C to 0°C and then dropping from 0°C to 25°C for both samples. The transition becomes less obvious with increasing frequency. The ε' variation with increasing frequency is determined by the ability of the dipoles in the

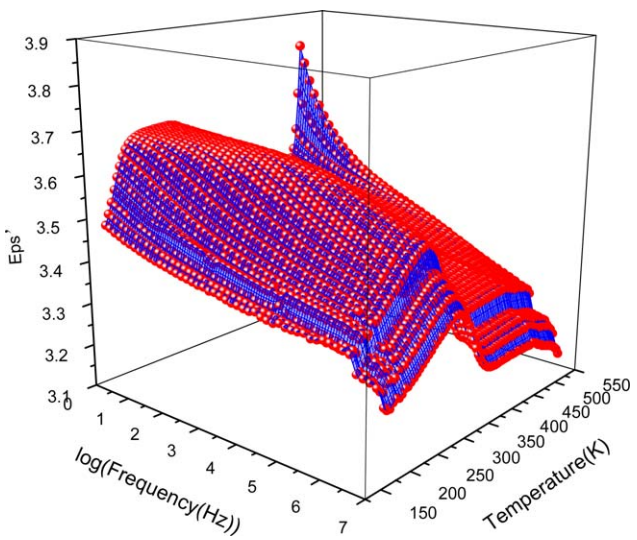

Figure 8. The dielectric constant versus frequency and temperature for ArPI-4. [Color figure can be viewed in the online issue, which is available at wileyonlinelibrary.com.]

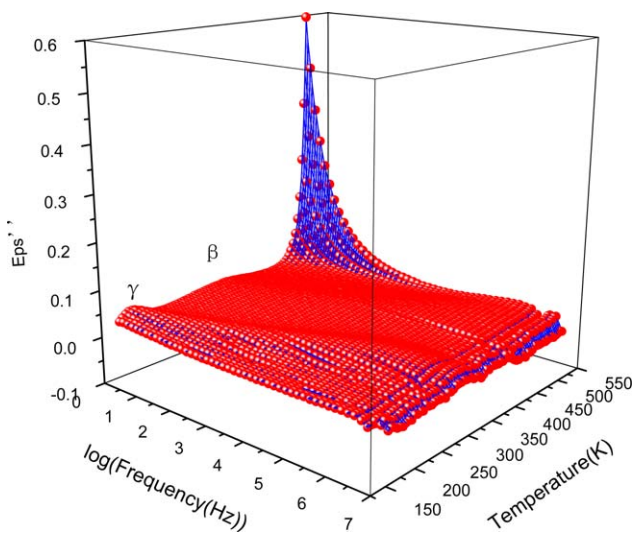

Figure 10. Dielectric loss versus frequency and temperature for CPI-4. [Color figure can be viewed in the online issue, which is available at wileyonlinelibrary.com.]

Table III. Dielectric Constant and Dielectric Loss of CPI-4 and ArPI-4 with Varied Frequency at 25°C

	Dielectric constant (ε')				Dielectric loss (ε'')	
Polymer	1 Hz	1000 Hz	1 MHz	10 MHz	1 Hz	1000 Hz
CPI-4	3.54	3.46	3.34	3.21	0.013	0.0064
ArPI-4	3.61	3.57	3.49	3.36	0.026	0.013

polymer to move fast enough to keep their orientation up with the increased oscillations of an alternating electric field. As the frequency increases, the orientational polarization of the dipoles would gradually lose pace with the changing frequency of the applied electric field, and so the dielectric constant ε' of the polymer begins to decrease. The decreasing tendency of ε' value with increasing frequency is reflected in all the curves in Figure 9. As the frequency of the applied electric field further increases to a certain value, the orientational polarization of the dipoles would eventually be out of the pace of the alternate electric field totally and become stagnant, and that signifies the minimum ε' (also referred to as ε'_∞).[42] Therefore, for each polymer with an established structure, the ε' values at different temperatures become convergent towards the minimum ε' with increasing frequency, as revealed by both CPI-4 and ArPI-4 and in Figure 9. That explains the less obvious transition of ε' versus temperature with increasing frequency for both samples. It is also clearly shown in Figure 9 that the Cardo-type polymer enjoys lower dielectric constant (ε') than the aromatic analog. The alicyclic cyclopentyl Cardo structure contributes to both larger free volume due to its bulky steric effect and lower polarizability of steric sp^3 hybridized carbon skeleton of cyclopentyl ring than the analogous planar sp^2 hybridized carbon skeleton of aromatic ring. In addition, the better hydrophobicity of CPI-4 leads to lower water absorption and thus the reduced dielectric constant, which provides a guarantee on long-term signal transmission reliability for its application to advanced microelectronic, such as flexible printed circuit board (FPCB).

Even though ε'' remains substantially stable over the most of measurement range, one can see some subtle relaxation on the plot of ε'' with variation of frequency and temperature. As shown in Figure 10, γ and β transition are discernible that are attributed to phenyl ring oscillations at low temperature and rotation of phenyl group and imide rings around hinges such as —O— linkages.[43] Apart from that, ε'' variation with temperature and frequency generally follows the similar tendency to that of ε', that is, ε'' value increases with increasing temperature and decreasing frequency.

A general comparison of dielectric properties under varied frequency at 25°C between CPI-4 and ArPI-4 was shown in Table III. Compared with traditional aromatic ArPI-4 (ODPA-ODA), Cardo-type CPI-2 (BDPCP-ODA) shows lower dielectric constant (ε') and thus displays better potential for microelectronic application as the signal propagation velocity and fidelity are inversely related to the dielectric constant of the insulating material.[32] Meanwhile, lower values of the dielectric loss (ε'') of the CPI-4 indicate less power dissipation and electric signal loss in the dielectric material. The presence of alicyclic cyclopentyl Cardo structure offers less polarizability, bigger free volume than aromatic ring does. Besides, CTC is inhibited by the introduction of alicyclic cyclopentyl structure. All these effects together result in advantageous dielectric properties of Cardo-type PI films for practical microelectronic application.

CONCLUSIONS

A novel unfunctionalized symmetric Cardo-type dianhydride monomer BDPCP containing the alicyclic cyclopentyl group with ester linkage was readily prepared via two facile steps in total purified yield of 61.1%. Comparative investigations between the BDPCP-derived Cardo-type polyimides CPI-*x* and the analogous ODPA-derived aromatic polyimides ArPI-*x* were performed to explore the structure–property relationship for practical application. It was found that the incorporation of the alicyclic cyclopentyl structure not only leads to the better solubility, higher optical transparence, decreased water absorption, increased hydrophobicity, but retains the inherent good mechanical properties and thermal stability owing to the moderate strain of cyclopentyl ring and inhibited CTC. In general, the lower dielectric constant and dielectric loss of Cardo-type polyimides revealed by dynamic dielectric measurement, together with higher optical transparence and comparable thermal and mechanical properties provide this readily accessible dianhydride with stronger competitiveness than traditional aromatic dianhydride for thin film optoelectronics and microelectronics application.

ACKNOWLEDGMENTS

The financial supports from the NSFC (Grant Nos. 51263014, 21271099, and 50803026), the Major State Basic Research Development Program (Grant No. 91022031), and Jiangxi Provincial Education Department (Grant No. GJJ13113) are greatly appreciated. The authors are thankful to Prof. Haoqing Hou from Jiangxi Normal University, China for kindly providing DMA measurements of all these samples.

REFERENCES

1. Wilson, D.; Stenzenberger, H. D. Polyimides-Chemistry and Application; Blackie and Sons, Ltd.: New York, **1990**.
2. Ding, M. X. *Prog. Polym. Sci.* **2007**, *32*, 623.
3. Hasegawa, M.; Horie, K. *Prog. Polym. Sci.* **2001**, *26*, 259.
4. Ree, M.; Kim, K.; Woo, S. H.; Chang, H. *J. Appl. Phys.* **1997**, *81*, 698.
5. Ando, S.; Matsuura, T.; Sasaki, S. *Polym. J.* **1997**, *29*, 69.
6. Wang, C. S.; Leu, T. S. *Polymer* **2000**, *41*, 3581.

7. Ma, T.; Zhang, S. J.; Li, Y. F.; Yang, F. C.; Gong, C. L.; Zhao, J. *J. Fluorine Chem.* **2010**, *131*, 724.
8. Shao, Y.; Li, Y. F.; Zhao, X.; Ma, T.; Gong, C. L.; Yang, F. C. *Eur. Polym. J.* **2007**, *43*, 4389.
9. Kim, H. S.; Kim, Y. H.; Ahn, S. K.; Kwon, S. K. *Macromolecules* **2003**, *36*, 2327.
10. Eastmond, G. C.; Paprotny, J. *J. Mater. Chem.* **1997**, *7*, 589.
11. Liu, F.; Wang, Z.; Yang, H. L.; Gao, L. X.; Ding, M. X. *Polymer* **2006**, *47*, 937.
12. Popovici, D.; Hulubei, C.; Cozan, V.; Lisa, G.; Bruma, M. *High Perform. Polym.* **2012**, *24*, 194.
13. Mathews, A. S.; Kim, I.; Ha, C. S. *J. Appl. Polym. Sci.* **2006**, *102*, 3316.
14. Zhang, H. S.; Li, J.; Tian, Z. L.; Liu, F. *J. Appl. Polym. Sci.* **2013**, *129*, 3333.
15. Hasegawa, M.; Kasamatsu, K.; Koseki, K. *Eur. Polym. J.* **2012**, *48*, 483.
16. Liu, J. G.; He, M. H.; Zhou, H. W.; Qian, Z. G.; Wang, F. S.; Yang, S. Y. *J. Polym. Sci. Polym. Chem.* **2002**, *40*, 110.
17. Watanabe, Y.; Sakai, Y.; Shibasaki, Y.; Ando, S.; Ueda, M. *Macromolecules* **2002**, *35*, 2277.
18. Matsumoto, T.; Kawabata, S.; Takahashi, R. *High Perform. Polym.* **2006**, *18*, 719.
19. Tapaswi, P. K.; Choi, M. C.; Jung, Y. S.; Cho, H. J.; Seo, D. J.; Ha, C. S. *J. Polym. Sci. Polym. Chem.* **2014**, *52*, 2316.
20. Biolley, N.; Grégoire, M.; Pascal, T.; Sillion, B. *Polymer* **1991**, *32*, 17.
21. Yi, M. H.; Huang, W. X.; Jin, M. Y.; Choi, K. Y. *Macromolecules* **1997**, *30*, 5606.
22. Laiw, D. J.; Chen, I. W.; Yang, M. C. *Macromol. Chem. Phys.* **2002**, *203*, 2170.
23. Yang, C. P.; Chen, R. S.; Yu, C. W. *J. Appl. Polym. Sci.* **2001**, *82*, 2750.
24. Liaw, D. J.; Huang, C. C.; Chen, W. H. *Macromol. Chem. Phys.* **2006**, *207*, 434.
25. Jin, X. Z.; Ishii, H. *J. Appl. Polym. Sci.* **2005**, *98*, 15.
26. Hsiao, S. H.; Li, C. T. *J. Polym. Sci. Polym. Chem.* **1999**, *37*, 1435.
27. Chenar, M. P.; Soltanieh, M.; Matsuura, T.; Tabe-Mohammadi, A.; Sadeghi, M. *J. Membr. Sci.* **2008**, *324*, 85.
28. Chenar, M. P.; Savoji, H.; Soltanieh, M.; Matsuura, T.; Tabe, S. *Korean J. Chem. Eng.* **2011**, *28*, 902.
29. Hamciuc, C.; Hamciuc, E.; Ipate, A. M.; Cristea, M.; Okrasa, L. *J. Appl. Polym. Sci.* **2009**, *113*, 383.
30. Kumar, R. S.; Ariraman, M.; Alagar, M. *RSC Adv.* **2014**, *4*, 19127.
31. Margelefsky, E. L.; BendjeÇriou, A.; Zeidan, R. K.; Dufaud, V.; Davis, M. E. *J. Am. Chem. Soc.* **2008**, *130*, 13442.
32. Maier, G. *Prog. Polym. Sci.* **2001**, *26*, 3.
33. Ghosh, M. K.; Mittal, K. L.; Eds. Polyimide: Fundmentals and Applications; Marcel Dekker, Inc.: New York, **1996**, Chapter 24, p 759.
34. Liaw, D. J.; Liaw, B. Y.; Lai, S. H. *Macromol. Chem. Phys.* **2001**, *202*, 807.
35. Laiw, D. J.; Hsu, C. Y.; Laiw, B. Y. *Polymer* **2001**, *42*, 7993.
36. Yang, C. P.; Su, Y. Y.; Hsiao, F. Z. *Polymer* **2004**, *45*, 7529.
37. Wang, X.; Liu, F.; Lai, J.; Fu, Z.; You, X. *J. Fluorine Chem.* **2014**, *164*, 27.
38. Yang, C. P.; Yu, C. W. *J. Polym. Sci. Polym. Chem.* **2001**, *39*, 788.
39. Carey, F. A.; Sundberg, R. J. Advanced Organic Chemistry; Spring Science & Business Media: New York, **2000**; Chapter 3, p 171.
40. Ebisawa, S.; Ishii, J.; Sato, M.; Vladimirov, L.; Hasegawa, M. *Eur. Polym. J.* **2010**, *46*, 283.
41. Fukukawa, K. I.; Okazaki, M.; Sakata, Y.; Urakami, T.; Yamashita, W.; Tamai, S. *Polymer* **2013**, *54*, 1053.
42. Eastmond, G. C.; Paprotny, J.; Pethrick, R. A.; Santamaria-Mendia, F. *J. Appl. Polym. Sci.* **2015**, *132*, 41684.
43. Li, J.; Zhang, H. S.; Liu, F.; Lai, J. C.; Qi, H. X.; You, X. Z. *Polymer* **2013**, *54*, 5673.